Journal of Non-Crystalline Solids 674 (2026) 123919

Contents lists available at ScienceDirect

Journal of Non-Crystalline Solids

journal homepage: www.elsevier.com/locate/jnoncrysol

Realizing casting formation of 100 mm complex structure Vit1 metallic glass component over hundreds of grams

Lunyong Zhang [a,b,*], Xiyuan Chen [a,b], Xiuzhang Li [c], Hongyan Kang [d], Xianxing Wang [a,b], Jinglong Mi [a,b], Chaojun Zhang [a,b], Ruishuai Gao [a,b], Zhishuai Jin [a,b], Guanyu Cao [a,b], Hongxian Shen [a,b,*], Jun Yi [e], Juntao Huo [f], Minzhen Ma [g], Fuyang Cao [a,b,*], Jianfei Sun [a,b,*]

[a] School of Materials Science and Engineering, Harbin Institute of Technology, Harbin 150001, China
[b] National Key Laboratory of Precision Hot Formation, Harbin Institute of Technology, Harbin 150001, China
[c] Shenyang Vacuum Technology Institute Co., LTD. Shenyang, 110042, China
[d] AECC Harbin Dongan Engine Co., Ltd, Harbin 150060, China
[e] Center of Advanced Solidification Technology, Shanghai University, Shanghai, 200444, China
[f] Key Laboratory of Magnetic Materials and Devices, Ningbo Institute of Material Technology and Engineering, CAS, Ningbo 315201, China
[g] State Key Laboratory of Metastable Materials Science and Technology, Yanshan University, Qinhuangdao 066004, China

ARTICLE INFO

Keywords:
Bulk metallic glasses
Casted components
Large size and complex structure
Casting process optimization

ABSTRACT

Bulk metallic glasses (BMGs) have not been applied in engineering despite their great potential over the past few decades. The size and structural limitations in the formation of BMG components remain a bottleneck, which continues to be a significant challenge. This work overcomes that bottleneck by utilizing the advantages of counter-gravity casting technology, optimizing the casting processes, and successfully forming a Vit1 BMG bracket component with an outer diameter of 100 mm and a weight of 462 g. The results show that copper molds are not suitable for achieving a cooling rate higher than the critical rate required for glass transition in the entire component. Additional water cooling on the mold is necessary to achieve a sufficiently high cooling rate. Based on this, the melt pouring temperature, mold preheating temperature, and pressurization speed were carefully tuned to ensure complete filling of the mold cavity and stable melt flow during cavity filling. This work demonstrates that it is feasible to produce large-sized and complex BMG components by casting, paving the way for the large-scale application of BMGs in various fields.

1. Introduction

Bulk metallic glasses (BMGs) have attracted significant attention in science and technology over the past decades due to their great potential as a structural material that could replace traditional metallic materials [1,2], However, this potential has not yet been fully realized, as BMGs have never been formed into large-sized, fully glassy components with complex structures by casting, due to their limited glass-forming ability. So far, only wires, rods, plates and/or tiny complex structure samples were prepared [2]. Their geometry is simple in most cases and overall size is still limited, often at a scale <100 mm. Breaking such a bottleneck is urgently required to further develop bulk metallic glasses and enable their engineering applications.

The attempt to form bulk metallic glasses (BMGs) through casting has been ongoing for nearly three decades [1,3]. Vacuum suction casting and die casting are the most applied methods in practice so far, by which, ball bearings [4], watch frame [4], key [5], golf head [6], mobile phone frame [7], strain wave gears [8] were produced even though some samples still contained minor nanocrystalline phases. The structural characteristics of these BMG casting components simplify the melt flow and temperature fields, which has led to less emphasis on designing the casting processes. As a result, the flow and freezing/solidification behaviors of BMGs have remained an open question, which however is crucial for achieving the successful casting of large, complex BMG components. Because enough mold cavity filling ability of the melt is necessary to successfully form a casting component, which requires a low cooling rate to make sure adequate filling time before fully freezing. Oppositely, high enough cooling rate is requested to ensure fully

* Corresponding authors.
E-mail addresses: zhangly@hit.edu.cn (L. Zhang), hitshenhongxian@163.com (H. Shen), caofuyang@hit.edu.cn (F. Cao), jfsun_hit@263.net (J. Sun).

https://doi.org/10.1016/j.jnoncrysol.2025.123919
Received 6 October 2025; Received in revised form 8 December 2025; Accepted 9 December 2025
Available online 17 December 2025

vitrification. Thus, a contradiction is created in the cooling conditions required for casting large, complex BMG components. A balance in the casting process must be achieved.

Recently, some efforts have focused on this issue from the perspective of casting technology. Ma etc. firstly evaluated the fluidity and filling ability of $Zr_{41}Ti_{14}Cu_{12.5}Ni_{10}Be_{22.5}$ (Vit1) melt in a copper spiral mold and explored the correlations between the fluidity and pouring speed/temperature [9]. Furtherly, a model predicting the flow length of Zr-based BMG melt in vacuum suction casting was constructed, which shows that the fluidity length is monotonically increased with temperature, pressure, and runner diameter [10]. The flow length of the BMG melt is primarily affected by the cooling capacity of the mold [11]. Appropriate conditions must be met to achieve smooth filling for avoiding casting defects [10]. It was shown that, in traditional gravity pouring process, increasing melt overheat temperature significantly improves the fluidity of Vit1 BMG melt compared to mold preheating temperature. However, this comes at the cost of the vitrification degree [12].

On the other hand, recent studies have revealed that the freezing of Zr-based BMGs occurs in a narrow transition layer, following a freezing mode analogous to the 'layer-by-layer' solidification observed in crystalline metals with a narrow crystallization temperature range. This means that the freezing of BMG melt does not occur simultaneously [13]. This understanding is crucial for designing the casting process to avoid defects in BMG components. The effect of mold materials on the freezing process of BMGs was also investigated. It was found that refractory steel, pure graphite, and copper molds result in distinct instantaneous cooling rates of 45, 52, and 64 K/s, respectively, which in turn affect the microstructure of the samples [11]. Proper increasing the mold temperature improves the freezing time without affecting the vitrification of amorphous melt, thus optimal mold temperature could be beneficial to improve the internal temperature gradient and reduce the risk of component deformation or cracking, without obviously decreasing the vitrification degree [14].

Such investigations show that the freezing process of BMG melt can be engineering modulated to a certain extent, opening the possibility for casting large-sized, complex BMG components with optimized processes. In the present work, a Vit1 BMG bracket in a fully glassy state, approximately 100 mm in size and weighing over 400 *g*, was successfully fabricated using the vacuum counter-gravity casting technique with optimized process conditions. It proves the feasibility to cast large size complex BMG component with fully volume vitrification and advance the engineering applications of BMGs.

2. Experimental

Fig. 1a shows the geometry of the bracket component which has a maximum diameter Φ 100 mm, which is often made by steel and used as a part of some machines, for example a supporting basement. Accordingly, the three-dimensional model of the bracket was constructed for further casting process design by cavity filling flow field and freezing temperature field simulations on the platform ProCAST 2022 with a numerical model shown as Fig. 1b which contains a copper mold cavity with outer dimensions 150 × 150 × 100 mm^3, 200× 200 × 110 mm^3 or 250× 250 × 120 mm^3 respectively. A melt rising tube as also shown in Fig,1b was set under the "thick and big" part of the component according to the pouring system design principle of casting technology. The melt filling pressuring process is vital and can be artificially controlled in counter-gravity casting, and so is necessary to be optimized by simulations. The filling pressuring process for simulation was shown in Fig. 1c, which was divided into three stages, the melt rising stage (I), the cavity filling stage (II) and the freezing stage under pressure (III). The first two stages are critical for realizing stable flow of melt and so decreasing casting defects like the gas and/or slug inclusions. The pressurization speed process was defined by the speed at the melt rising stage and the cavity filling stage. During the freezing temperature field simulations, three points were set on the casting as noted in Fig. 1d for probing temperature evolution. The point 1 was chosen at the upper fringe of the casting. The point 2 and 3 were chosen at the "thick and big" part where should be the finally frozen region and cooled slowest. For simulating the air cooling condition, the heat exchange coefficient between mode and environment is set as 20 W/(m^2·K), environment temperature is 20 ℃. For simulating the water cooling condition, the heat exchange coefficient between mode and environment is set as 5000

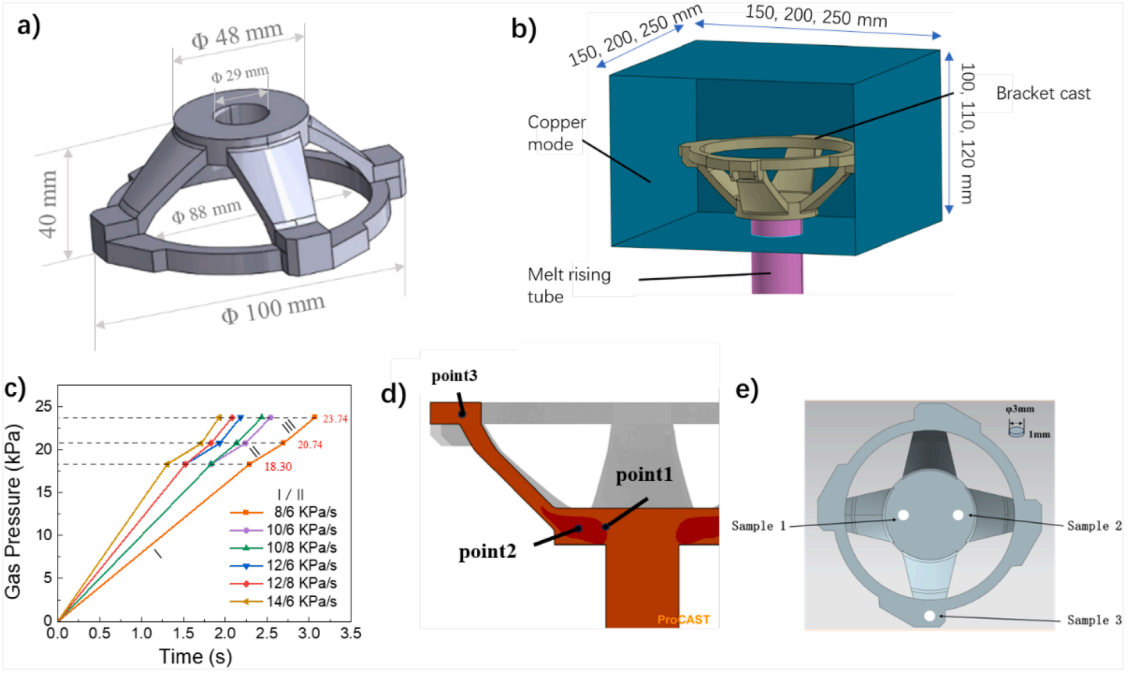

Fig. 1. Experimental conditions. a) casting structure; b) three-dimensional model for casting process simulation, cooper molds with size 150×150×100 mm^3, 200×200×110 mm^3 and 250×250×120 mm^3 were studied respectively; c) antigravity casting pressuring processes; d) Temperature extracting point during casting simulations; e) Places for cutting the XRD samples on the casting.

W/(m^2·K), environment temperature is 15 ℃.At last, three small blocks were cut from the casting sample from three places as indicated in Fig. 1e. The X-ray diffraction (XRD) measurement was carried out on a XPERT PRO XRD machine with Cu-Kα course (λ=1.540 Å). The casting was scanned layer by layer from the top to bottom along the cavity filling direction by an industrial computerized tomography system (model AX2000, Aoyun Electronic Technology Co., Ltd., Xi'an, China). The step length is 1 mm.

3. Results and discussions

We firstly explored the effects of copper mold dimensions on the component casting process. Fig. 2 demonstrates the temperature field evolution during the pouring and freezing of melt. It was shown that the melt reached the middle part of four ribbed plates of the bracket after filling for 2.32 s, for all the molds (the left column of Fig. 2). The primary difference observed was in the temperature distribution. The smallest dimensional mold supports the highest melt temperature after filled in the mold, exceeding 1121 ℃ at most parts of the component, except for the bottom near the inner pouring outlet, where the melt/mold contact area is relative larger. In contrast, the melt temperature in the larger molds was consistently lower than 1121 °C, with the temperature decreasing further as the mold size increased. This is consistent with traditional expectations, where larger metal molds generally provide better cooling effects, but beyond a certain mold size, the cooling effect becomes less influenced by mold dimensions.

The cavity filling ability of melt is a key condition for successfully forming the component, which is almost determined by melt temperature for a given material composition. The temperature field evolution simulation results (Fig. 2) indicated that the mold cavity could be fully filled for all the three molds under air cooling conditions, even though the larger mold exhibited higher cooling rate (the middle and right column of Fig. 2). Fig. 3 further illustrates the freezing process of the casting, represented by the simulated solid fraction under air cooling conditions. Freezing is defined as starting when the temperature drops to the liquidus point (T_{liq} = 717 °C for Vit1 BMG) and finishing when the temperature reaches the solidus point (T_{sol} = 665 °C) [13]. The results show that freezing began at the upper thinnest part of the fringe ring (Fig. 4a), followed by freezing at the 4 p.m. connecting the upper ring to the lower part (Fig. 3b). Once the four connecting parts between the upper ring and arms froze, the lower part was the last to solidify (Fig. 3c). This freezing route could potentially cause porosity defects at the connections between the upper ring and the arms, based on casting theory. Fortunately, further results predicted that none such defects will form at the places, see Fig. 3d From this perspective, the pouring system design appears to be appropriate.

However, as regard to BMGs, cooling rate higher than the critical one is required for successful vitrification. This is explored in Fig. 4, showing the simulated temperature evolution behaviors during whole casting process with air cooling. Fig. 4a gives out the temperature evolution of the three probing points under air cooling condition. Point 1, located near the inner pouring outlet, shows the slowest temperature descent, which aligns with expectations based on traditional casting principles. The region noted by point 1 would be frozen finally and experiences the slowest cooling rate, making it most susceptible to failure in vitrification due to a cooling rate that is lower than the critical rate for vitrification.

So far, two methods have been introduced to estimate the occurring of vitrification of Vit 1 BMG through cooling rate. One method calculates the average cooling rate of the melt from 1000 °C to the glass transition temperature (T_g = 340 °C for Vit1 BMG)] [15,16], while the other method uses the cooling rate at the glass transition temperature itself [17]. The first method requires an average cooling rate higher than 7.2 °C/s for vitrification, while the second method sets the critical cooling rate at 1 °C/s, for the Vit1 BMG. As shown in Fig. 4b, the average cooling rates at point 1, calculated from the simulated temperature curves, are 4.34 ℃/s according to the first method for the cooper mold with

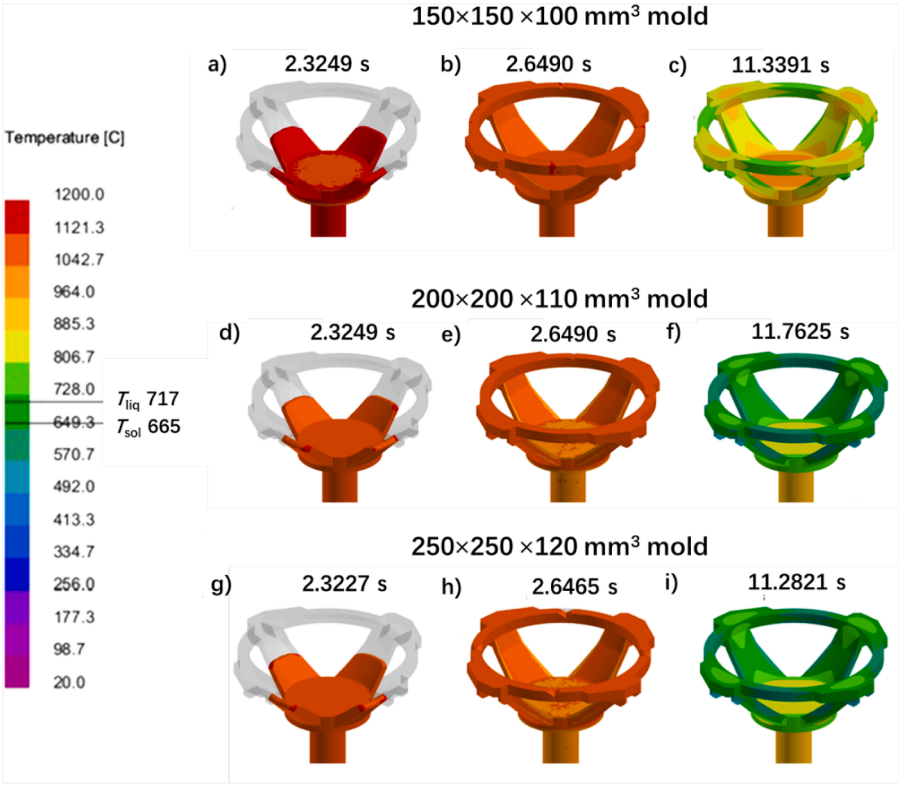

Fig. 2. Simulated temperature field evolution during melt filling and also freezing with different cooper mold dimensions. The filling pressuring process is 10/8 kPa/s. The pouring temperature is 1200 ℃ and the preheating temperature of rising tube is 700 ℃. The mold is not preheated and set at room temperature. Molds are not preheated.The T_{liq} and T_{sol} respectively represent the liquidus temperature and solidus temperature.

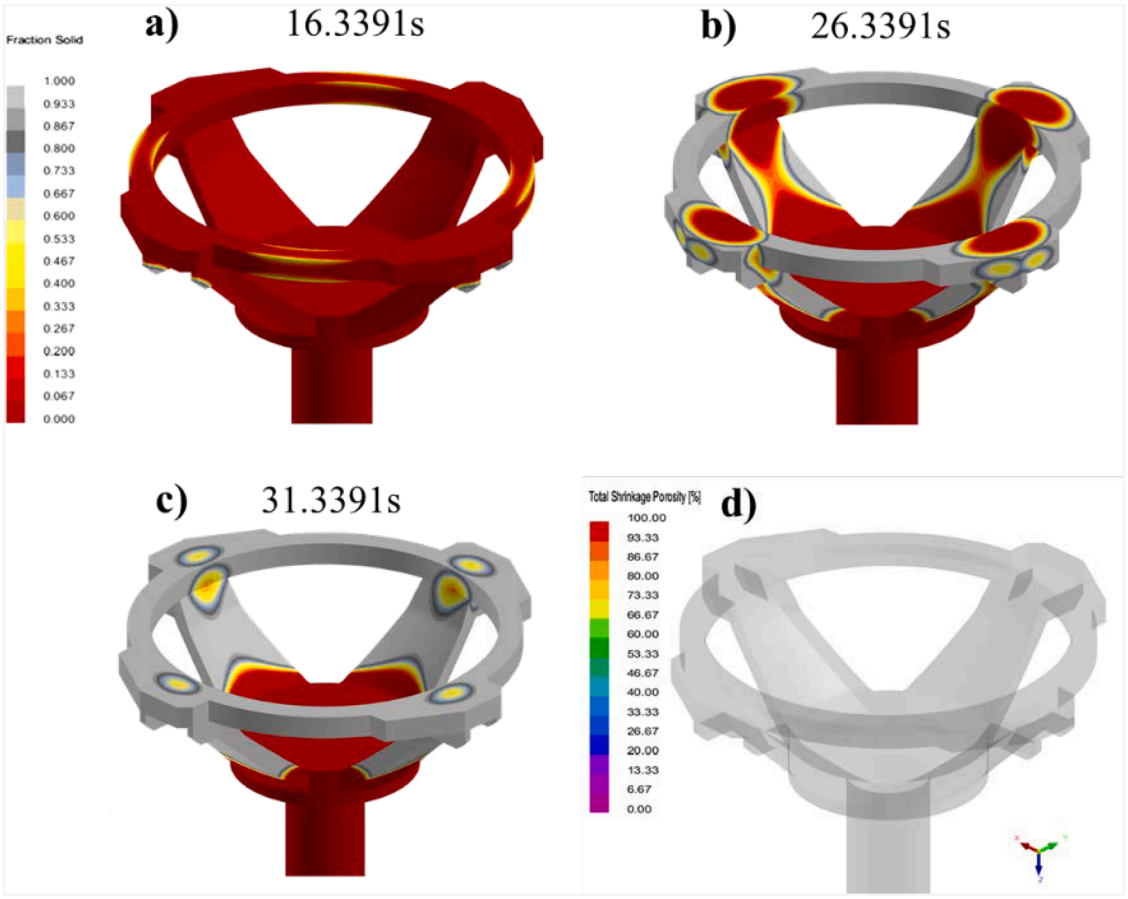

Fig. 3. Freezing fraction evolution a)-c) and defect prediction diagram d) under air cooling. The filling pressuring process is 10/8 kPa/s. The pouring temperature is 1200 ℃ and the preheating temperature of rising tube is 700 ℃.

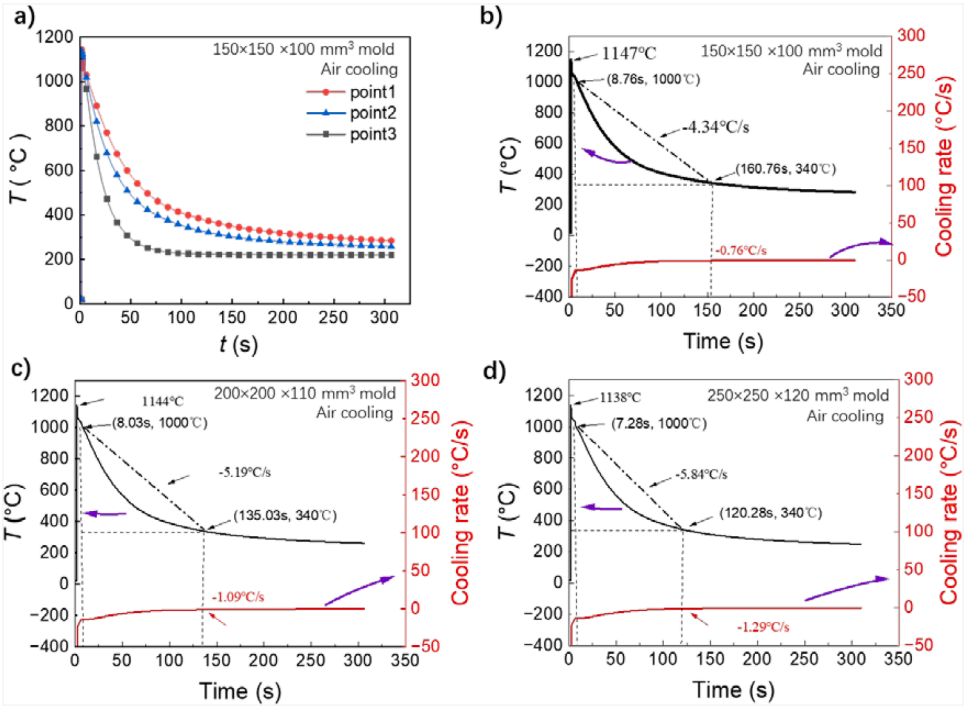

Fig. 4. Temperature evolution behavior at the probed points. a) temperature evolution at the probing points of the 150 × 150 × 100 mm^3 mold with air cooling; b)-d) show the temperature evolution and cooling rate at the probing point 1 of the molds of dimensions 150 × 150 × 100 mm^3, 200× 200 × 110 mm^3 and 250× 250 × 120 mm^3 respectively.

dimensions 150 × 150 × 100 mm^3. The cooling rates obtained at the glass transition point T_g are 0.76 ℃/s according to the second method. For the molds with dimensions 200× 200 × 110 mm^3 or 250× 250 × 120 mm^3, the average cooling rates are 5.19 °C/s and 5.84 °C/s, respectively, and the cooling rates at Tg are 1.09 °C/s and 1.29 °C/s, respectively. While the larger molds seem to produce a cooling rate at T_g slightly higher than the required critical rate of 1 °C/s, their average cooling rates are still below the critical average cooling rate of 7.2 °C/s required for full vitrification.

It is not expected that further increasing the cooling rate can be achieved by simply enlarging the copper mold size, as the improvement in cooling effect weakens with increasing mold size. This has already been demonstrated in molds with dimensions of 200 × 200 × 110 mm^3 and 250 × 250 × 120 mm^3. Additionally, larger copper molds increase costs. Therefore, we sought to optimize the casting process by introducing water cooling conditions instead of air cooling. Fig. 5 shows the temperature evolution during melt filling and freezing in a copper mold with dimensions 150 × 150 × 100 mm^3, under both air cooling (Fig. 5a–d) and water cooling (Fig. 5e–h). In general, the melt filling speed does not appear to be significantly affected by the cooling conditions of the copper mold. However, the cooling rate after the cavity is fully filled is influenced by the cooling conditions. Water cooling seems to offer a higher cooling rate, as shown in Fig. 6a. It was found that applying water cooling to the copper mold significantly improves its cooling effect. The average cooling rate in the temperature ranges from 1000 °C to the glass transition temperature (Tg) of Vit1 BMG is 7.76 °C/s, while the cooling rate at the Tg point is 3.25 °C/s. Water cooling helps remove heat from the copper mold, suppressing the temperature rise and enhancing the mold's cooling effect.

On the other hand, as seen from Fig. 6b, freezing began at 25.53 s and finished at 35.53 s under water cooling at the point 1. For air cooling, freezing started at 96.34 s and finished at 135.53 s. The melt freezes much faster under water cooling condition. Thus, air cooling alone, even with a copper mold, cannot provide a sufficient cooling rate to ensure vitrification of the Vit1 BMG melt at this volume and wall thickness scale for a complex structure component. This is contrast to the casting of traditional small BMGs rods or plate samples, where a thick cooper mold is typically sufficient to achieve the required cooling rate for full-volume vitrification. Thus, addition water-cooling is both suitable and necessary to realize the vitrification for the current bracket component. Accordingly, the following process investigations were carried out under water cooling condition.

We further optimized the pouring temperature to achieve the best balance between cooling rate and mold filling ability. The upper panel of Fig. 7 illustrates the mold cavity filling in a water-cooled 150×150×100 mm^3 mold at a pouring temperature of 1000 °C, with varying pressurization speeds. At a pressurization speed of 10/6 kPa/s, a significant portion of the cavity near the upper fringe remained unfilled because the melt temperature decreased too much, reducing flowability before the cavity was fully filled. When the pressurization speed during the cavity filling stage was increased from 6 kPa/s to 8 kPa/s, the unfilled cavity volume was significantly reduced (Fig. 7b). Increasing the pressurization speed during the melt rising stage by the same 2 kPa/s also slightly improved the filling rate (Fig. 7c), though the effect was less significant compared to the cavity filling stage. The cavity was fully filled at a pressurization speed of 12/8 kPa/s, but could not be completely filled at 14/6 kPa/s. Therefore, the optimized pressurization speed for this component was determined to be 12/8 kPa/s.

Then, the flow field must be investigated also to realize stable flow as much as possible because melt turbulence would involve gas in melt and increase the porosity in the final casting. The lower panel of Fig. 7 shows the melt flow filed dependent on filling time under the pressurization speed process 12/8 kPa/s. It was shown that the melt does not smoothly flow out from the inner outlet of the melt rising tube, but undergoes fluid jet like a fountain at some extent (Fig. 7f), which causing a lateral overflow (Fig. 7g) and further vortex flow at the corner of the inner outlet (Fig. 7h). The vortex becomes larger with time elapse (Fig. 7i). Such vortex flow would involve and intercept gas bubble or slags, should be avoided as possible. The cavity filling rate and melt flow field were simulated as well at pouring temperature 1200 ℃ and 1400 ℃, at different pressurization speed processes (Fig. 8). It was shown that a small part at the fringe of the component is still not filled at pouring

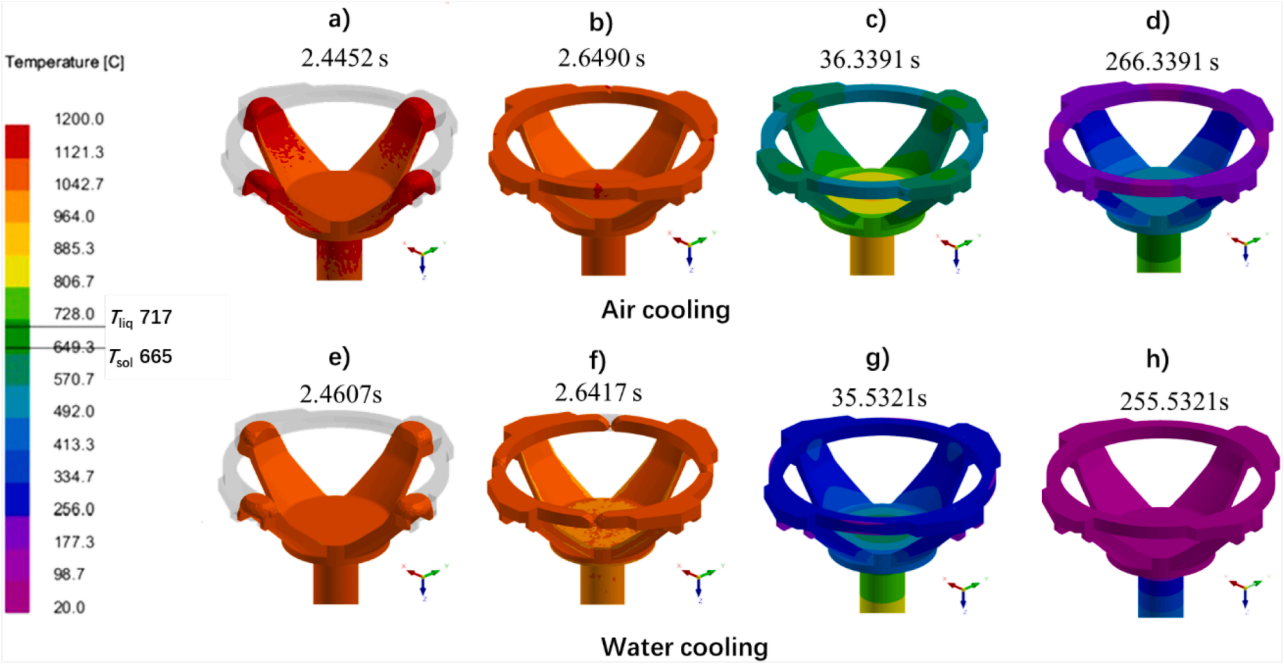

Fig. 5. Simulated temperature field evolution during melt filling and also freezing with different cooling conditions. The copper mold is 150×150×100 mm^3. Upper panel for air cooling condition and lower panel for water cooling. The filling pressuring process is 10/8 kPa/s. The pouring temperature is 1200 ℃ and the preheating temperature of rising tube is 700 ℃. The T_{liq} and T_{sol} respectively represent the liquidus temperature and solidus temperature. Molds are not preheated.

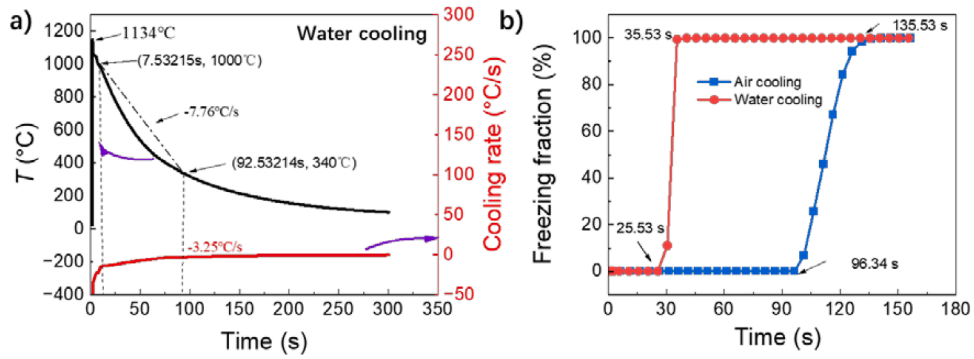

Fig. 6. Temperature evolution behavior at the probed point 1 for the mold of dimensions 150 × 150 × 100 mm^3 under water cooling. a) the temperature evolution and cooling rate; b) comparison of freezing fraction evolution at the point 1, under air cooling and water-cooling conditions.

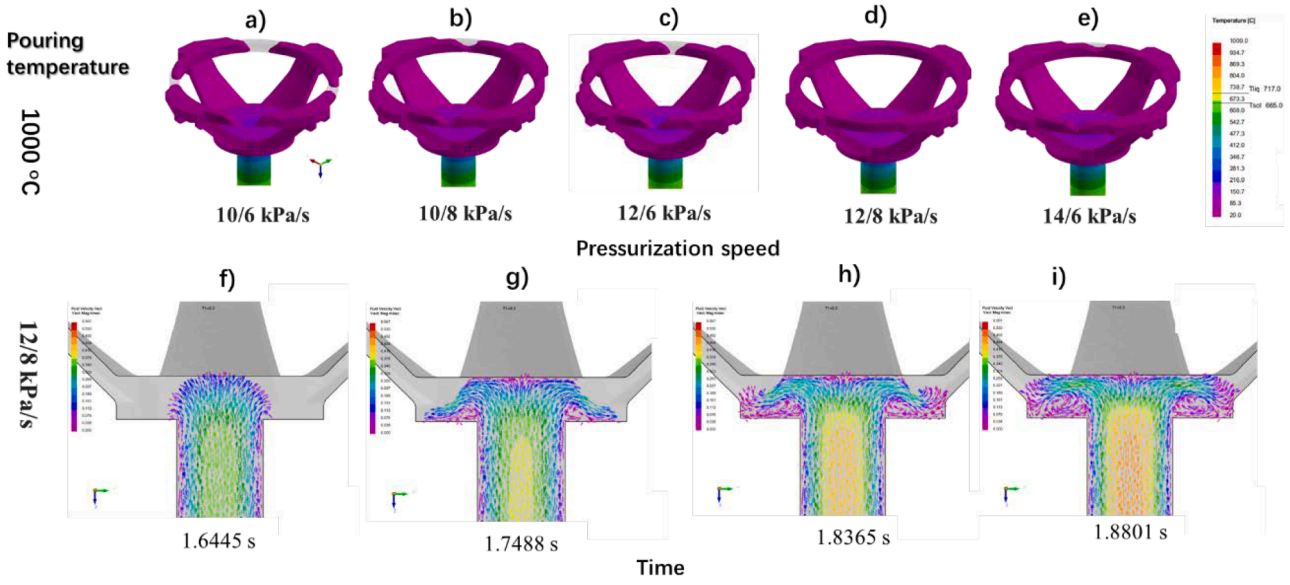

Fig. 7. Mold cavity filling and melt flow field in the water cooled 150×150×100 mm^3 mold with pouring temperature 1000 ℃ and different pressurization speed process. Upper panel shows the cavity filling and lower panel shows the follow filed. The preheating temperature of rising tube is 700 ℃. Mold is not preheated.

temperature 1200 ℃ by using pressurization speed process 8/6 kPa/s (Fig. 8a), whereas it can be fully filled by using pressurization speed process 10/6 kPa/s (Fig. 8b). Then, Fig. 8e and f indicate that the mold cavity could be fully filled by melt when pouring temperature is chosen as 1400 ℃ even at a relatively small pressurization speed process 6/4 kPa/s and 8/6 kPa/s. On the other hand, the flow filed simulations indicated that lateral overflow and weak vortex flow still exist at pouring temperature 1200 ℃ with pressurization speed process as 10/6 kPa/s (Fig. 8c and d). In contrast, the vortex flow is very strong when the pouring temperature is 1400 ℃ and pressurization speed process is 6/4 kPa/s (Fig. 8h), even though its lateral overflow is weak (Fig. 8g).

It has demonstrated that only a weak vortex flow is formed when the pressurization speed process is 10/6 kPa/s (Fig. 8d) and the unfilled volume is very small at pressurization speed process is 8/6 kPa/s (Fig. 8a), at pouring temperature 1200 ℃. Thus, the optimal casting process is nearly achieved. We expect to remove the small gap by slightly preheating the copper mold. Fig. 9 gives out the simulated cavity filling rate and also cooling rate in the 150×150×100 mm^3 mold, with a pouring temperature of 1200 ℃ and pressurization speed process of 8/6 kPa/s, at different mold preheating temperatures. In general, copper mold preheating improves melt filling ability and the mold cavity could be fully filled for all cases with preheating temperature as 200 ℃, 400 ℃ and 600 ℃ (Fig. 9a–c). Correspondingly, the temperature evolution and cooling rate at the probing point 1 show that the average cooling rate reaches 13.42 ℃/s, 10.37 ℃/s and 6.47 ℃/s, respectively for the case of mold preheating temperature as 200 ℃, 400 ℃ and 600 ℃. The cooling rate at T_g is 4.06 ℃/s, 3.33 ℃/s and 2.93 ℃/s, respectively. Thus, the average cooling rate for the case of 600 ℃ does not meet the glass transition requirement, while the other two cases with preheating temperatures of 200 ℃ and 400 ℃ are applicable to cast the current Vit1 BMG component.

With above optimization of casting processes, we carried out practical casting of the bracket component by using the precise counter-gravity casting apparatus for large size amorphous alloys we developed recently, as shown in Fig. 10a. The casting process parameters were set as follows: melt pouring temperature of 1200 °C, melt rising tube preheating temperature of 700 °C, mold preheating temperature of 400 °C, and a pressurization speed process of 8/6 kPa/s. The cross-sectional image of the copper mold with the water-cooling pipeline is shown in Fig. 10b in three dimensions, with approximate dimensions of 150 × 150 × 100 mm^3. We finally obtained Vit1 BMG bracket castings for instance showing in Fig. 10c. The casting is fully formed and exhibits the bright metallic luster typically seen in BMG samples. The bracket casting weighs 462.9 g. Further XRD characterizations were carried out on three samples cut from the casting on the places shown in Fig. 1e, and the obtained XRD patterns were depicted in Fig. 10e. Obviously, all XRD

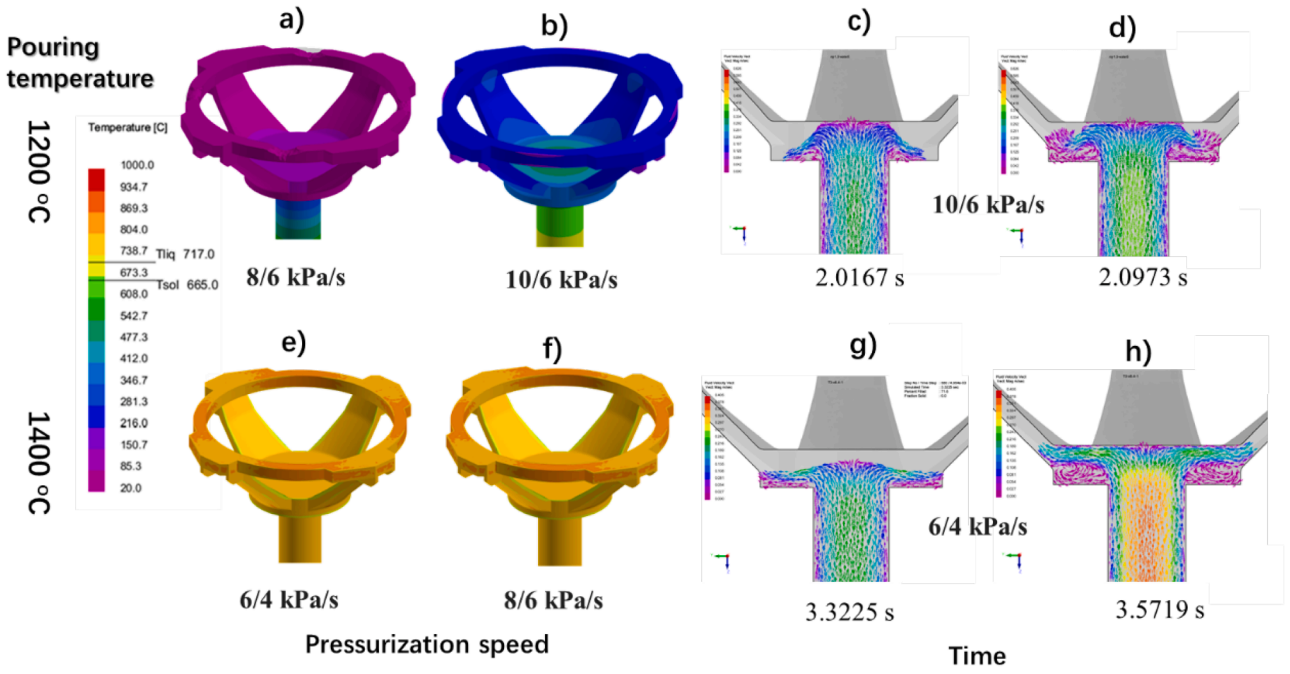

Fig. 8. Mold cavity filling and melt flow field in the water cooled 150×150×100 mm^3 mold with pouring temperature 1200 ℃ and 1400 ℃ at different pressurization speed process. The upper panel lists the results simulated at pouring temperature 1200 ℃ and the lower panel lists the results at 1400℃.

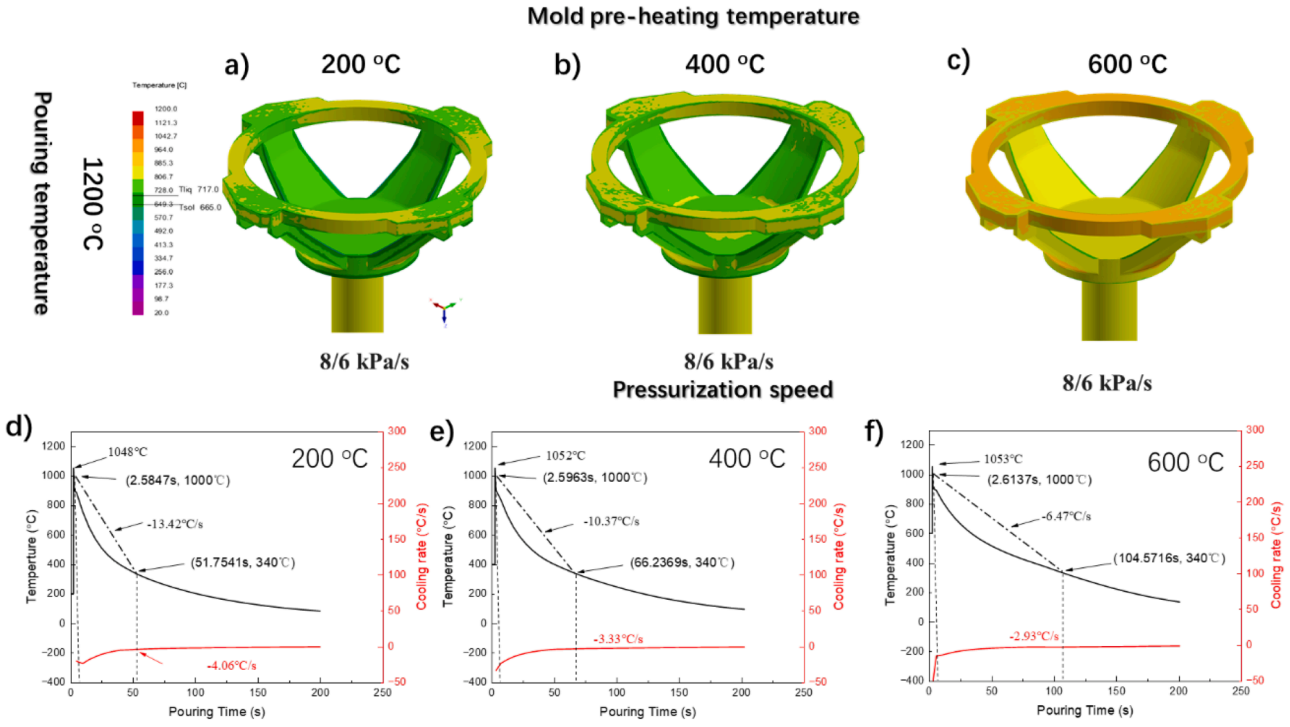

Fig. 9. Optimizing the mold-preheating temperature by simulating a)-c) the mold cavity filling rate and d)-f) cooling rate under different preheating temperatures. The mold dimensions are 150×150×100 mm^3, and pouring temperature is 1200 ℃. The pressurization speed process as 8/6 kPa/s. Melt rise tube is preheated at 700 ℃.

spectra clearly show a single diffused broad peak at $2\theta \sim 38°$, indicating that all samples cut from the casting are in the glass state. Fig. 3a–c have shown that the bottom of the casting, which contains samples 1 and 2, froze last and had the lowest cooling rate, thus the confirmed glass state of the samples 1 and 2 at the bottom, as well as the sample 3 at the upper fringe, ensures that entire casting is in a fully glassy state. Additionally, cross-sectional images of the casting, obtained through computed tomography, clearly reveal that the casting has good internal quality (Fig. 11). Only four pores (see the images a7, b6, c2 and d3 in Fig. 11), each approximately 1 mm in diameter, were detected except a somehow longer pore in the inner pouring outlet (f3-f7 in Fig. 11), which would endow the casting with high mechanical performances.

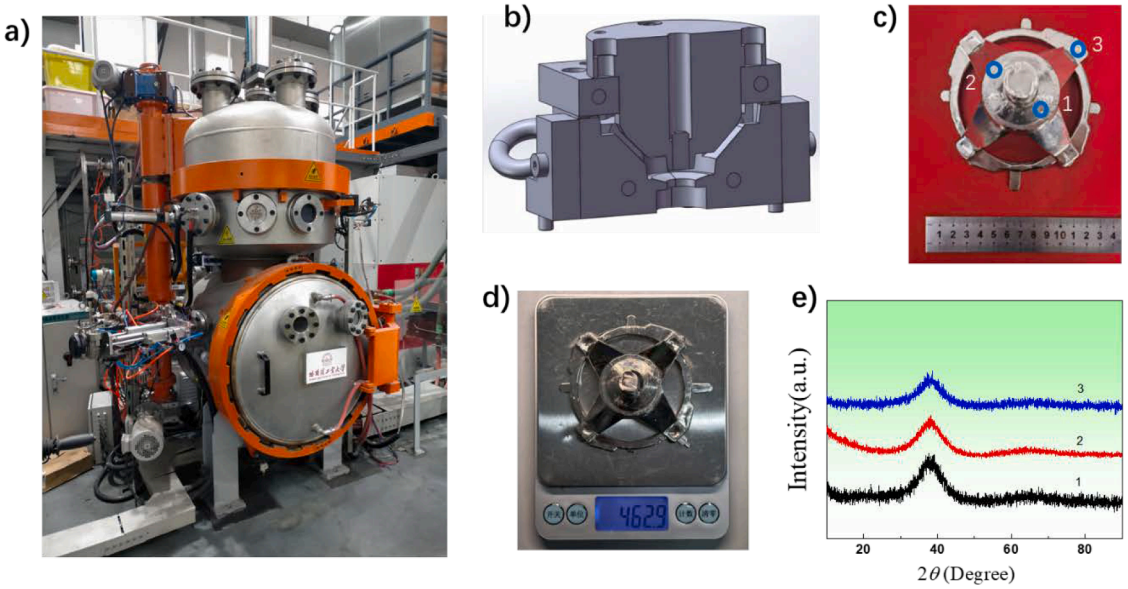

Fig. 10. Practically casting formation of the Vit1 BMG bracket component. a) shows the counter-gravity casting apparatus used for casting the component; b) the cross-section image of the cooper mold with water cooling pipeline; c) the component casting picture; d) the weight of the component casting; e) XRD patterns of three samples cut from the casting at the places shown in Fig. 1e.

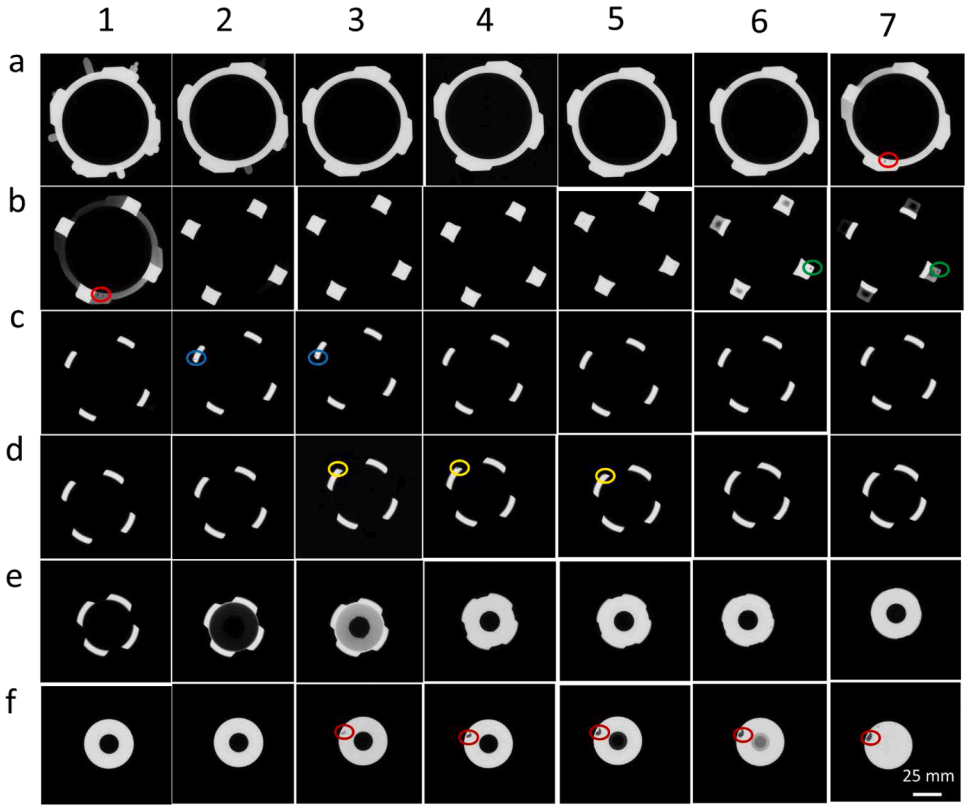

Fig. 11. CT Cross-section images of the bracket casting. The imaging section is perpendicular to cavity filling direction and the measurement step is 1 mm. The circles note the pores. Images a7 and b1 note one pore, b6 and b7 note one, c2 and c3 note one, d3-d5 note one, f3-f7 note one.

4. Conclusions

In summary, we successfully cast a large size bracket component with complicate structure and minor pores by using counter-gravity precision casting technology based on intricate optimization of the casting processes to ensure complete structural formation and full-volume vitrification. Our results showed that water cooling is essential to enhance the cooling effect of the copper mold and achieve the critical cooling rate required for glass transition. Once the critical cooling rate is met, the filling speed, the pouring temperature and the mold preheating temperature should be optimized collaboratively. Increasing pressurizing speed could enhance cavity filling efficiency but too high speed would cause melt flow turbulence. Increasing the pouring temperature and mold preheating temperature could improve the filling ability of

melt, but they cannot be too high to avoid decreasing the cooling rate lower than the critical value. It is recommended to maintain a high melt temperature to ensure adequate flowability, which is crucial for fully filling the mold cavity at a low filling speed, on the premise of meeting the full-volume vitrification conditions.

Data statement

The data that support the findings of this study are available from the corresponding author upon reasonable request.

CRediT authorship contribution statement

Lunyong Zhang: Writing – review & editing, Writing – original draft, Visualization, Validation, Supervision, Project administration, Funding acquisition, Formal analysis, Data curation, Conceptualization. **Xiyuan Chen:** Writing – original draft, Validation, Software, Investigation, Formal analysis. **Xiuzhang Li:** Resources, Investigation. **Hongyan Kang:** Resources, Investigation. **Xianxing Wang:** Software, Investigation. **Jinglong Mi:** Software, Investigation. **Chaojun Zhang:** Resources, Investigation. **Ruishuai Gao:** Software, Investigation. **Zhishuai Jin:** Software, Investigation. **Guanyu Cao:** Software, Investigation. **Hongxian Shen:** Writing – review & editing, Validation, Supervision, Project administration, Formal analysis, Data curation. **Jun Yi:** Writing – review & editing, Validation, Funding acquisition, Conceptualization. **Juntao Huo:** Writing – review & editing, Validation, Funding acquisition, Conceptualization. **Minzhen Ma:** Writing – review & editing, Validation, Funding acquisition, Conceptualization. **Fuyang Cao:** Writing – review & editing, Validation, Supervision, Project administration, Methodology, Formal analysis, Data curation. **Jianfei Sun:** Writing – review & editing, Validation, Supervision, Project administration, Funding acquisition, Conceptualization.

Declaration of competing interest

The authors declare that they have no known competing financial interests or personal relationships that could have appeared to influence the work reported in this paper.

Ackowledgements

This work was supported by the National Natural Science Foundation of China (Grant number 52471172, 52371152, 51827801).

References

[1] K. Gao, X.G. Zhu, L. Chen, W.H. Li, X. Xu, B.T. Pan, W.R. Li, W.H. Zhou, L. Li, W. Huang, Y. Li, Recent development in the application of bulk metallic glasses, J. Materials Sci. Technol. 131 (2022) 115–121.
[2] S. Sohrabi, J. Fu, L. Li, Y. Zhang, X. Li, F. Sun, J. Ma, W.H. Wang, Manufacturing of metallic glass components: processes, structures and properties, Prog. Mater. Sci. 144 (2024) 101283.
[3] R. LIU, M. MA, X.J.A.M.S. ZHANG, New development of research on casting of bulk amorphous alloys, Acta Metall. Sin 57 (2021) 515–528.
[4] D.C. Hofmann, S.N. Roberts, Microgravity metal processing: from undercooled liquids to bulk metallic glasses, NPJ Microgravity 1 (2015) 15003.
[5] P. Ramasamy, A. Szabo, S. Borzel, J. Eckert, M. Stoica, A.J.S.r. Bárdos, High pressure die casting of Fe-based metallic glass, Sci. Rep. 6 (2016) 35258.
[6] Y.C. Choi, S.I. Hong, Mechanical properties and microstructure of commercial amorphous golf club heads made of Zr–Ti–Cu–Ni–Be bulk metallic glass, Materials Sci. Eng.: A 449-451 (2007) 126–129.
[7] L. Liu, T. Zhang, Z. Liu, C. Yu, X. Dong, L. He, K. Gao, X. Zhu, W. Li, C.J.M. Wang, Near-net forming complex shaped Zr-based bulk metallic glasses by high pressure die casting, 11 (2018) 2338.
[8] D.C. Hofmann, R. Polit-Casillas, S.N. Roberts, J.-P. Borgonia, R.P. Dillon, E. Hilgemann, J. Kolodziejska, L. Montemayor, J.-o. Suh, A. Hoff, K. Carpenter, A. Parness, W.L. Johnson, A. Kennett, B. Wilcox, Castable bulk metallic glass strain wave gears: towards decreasing the cost of high-performance robotics, Sci. Rep. 6 (2016) 37773.
[9] M. Ma, H. Zong, H. Wang, Y. Qi, S. Liang, A. Song, W. Zhang, Q. Wang, X. Zhang, Q. Jing, G. Li, R. Liu, The fluidity and molding ability of glass-forming Zr-based alloy melt, Science in China Series G: physics, Mechan. Astron. 51 (2008) 438–444.
[10] D.-q. Ma, X.-z. Ma, H.-y. Zhang, M.-z. Ma, X.-y. Zhang, R.-p. Liu, Evaluation of casting fluidity and filling capacity of Zr-based amorphous metal melts, J. Iron Steel Res. Int. 25 (2018) 1163–1171.
[11] F. Wang, D. Yin, J. Lv, S. Zhang, M. Ma, X. Zhang, R. Liu, Effect of cooling rate on fluidity and glass-forming ability of Zr-based amorphous alloys using different molds, J. Mater. Processing Technology 292 (2021) 117051.
[12] G. Cao, Z. Wang, L. Zhang, Z. Jin, C. Zhang, R. Gao, Z. Qiu, Y. Li, Y. Dong, Y. Huang, F. Cao, H. Shen, J. Sun, Melt fluidity and microstructure of bulk metallic glass under different cooling conditions, J Alloys Compd 1015 (2025) 178869.
[13] Z. Jin, F. Cao, G. Cao, C. Zhang, Z. Qiu, L. Zhang, H. Shen, S. Jiang, Y. Huang, M. Ma, E. Jürgen, J. Sun, Effect of casting temperature on the solidification process and (micro)structure of Zr-based metallic glasses, J. Mater. Res. Technol. 22 (2023) 3010–3019.
[14] Z. Jin, C. Zhang, G. Cao, Z. Qiu, L. Zhang, H. Shen, S. Jiang, F. Cao, Y. Huang, M. Ma, P. Ramasamy, J. Eckert, J. Sun, Effect of mold temperature on the solidification process and microstructure of Zr-based metallic glasses during casting, J. Non Cryst. Solids 627 (2024) 122821.
[15] X.P. Tang, J.F. Löffler, W.L. Johnson, Y. Wu, Devitrification of the Zr41.2Ti13.8Cu12.5Ni10.0Be22.5 bulk metallic glass studied by XRD, SANS, and NMR, J. Non Cryst. Solids 317 (2003) 118–122.
[16] D. Peng, J. Sun, J. Shen, D. Chen, G. Wang, Y. Chen, Solidification thermodynamics of bulk amorphous $Zr_{41.2}$ $Ti_{13.8}$ $Cu_{12.5}$ Ni_{10} $Be_{22.5}$ alloy, Chin. J. Nonferrous Metals 13 (2003) 1083–1086.
[17] X. Tian, J. Shen, J. Sun, Y. Gao, G. Wang, Q. Li, C. Li, X. Chen, The thermo-physical properties for the bulk amorphous alloy and the numerical simulation during its cooling process, Special Casting & Nonferrous Alloys (2003) 23.